Published in final edited form as:
Glia. 2015 March ; 63(3): 452–465. doi:10.1002/glia.22764.

Transplanted Glial Restricted Precursor Cells Improve Neurobehavioral and Neuropathological Outcomes in a Mouse Model of Neonatal White Matter Injury Despite Limited Cell Survival

Michael Porambo[1], **Andre W. Phillips**[1,2], **Joel Marx**[1], **Kylie Ternes**[1], **Edwin Arauz**, **Mikhail Pletnikov**[3], **Mary Ann Wilson**[1,2,4], **Jeffery D. Rothstein**[2,4], **Michael V. Johnston**[1,2,5], and **Ali Fatemi**[1,2,5]

[1]Kennedy Krieger Institute, Johns Hopkins University

[2]Department of Neurology, Johns Hopkins University

[3]Department of Psychiatry, Johns Hopkins University

[4]Department of Neuroscience, Johns Hopkins University

[5]Department of Pediatrics, Johns Hopkins University

Abstract

Objective—Neonatal White Matter Injury (NWMI) is the leading cause of cerebral palsy and other neurocognitive deficits in prematurely-born children, and no restorative therapies exist. Our objective was to determine the fate and effect of glial restricted precursor cell (GRP) transplantation in an ischemic mouse model of NWMI.

Methods—Neonatal CD-1 mice underwent unilateral carotid artery ligation on postnatal-day 5 (P5). At P22, intracallosal injections of either eGFP+ GRPs or saline were performed in control and ligated mice. Neurobehavioral and postmortem studies were performed at four and eight weeks post-transplantation.

Results—GRP survival was comparable at one month but significantly lower at two months post-transplantation in NWMI mice compared to unligated controls. Surviving cells showed better migration capability in controls; however, the differentiation capacity of transplanted cells was similar in control and NWMI. Saline-treated NWMI mice showed significantly altered response in startle amplitude and pre-pulse inhibition paradigms compared to unligated controls, while these behavioral tests were completely normal in GRP-transplanted animals. Similarly, there was significant increase in hemispheric myelin basic protein density, along with significant decrease in pathologic axonal staining in cell-treated NWMI mice compared to saline-treated NWMI animals.

Interpretation—The Reduced long-term survival and migration of transplanted GRPs in an ischemia-induced NWMI model suggests that neonatal ischemia leads to long-lasting detrimental

Corresponding Author: Ali Fatemi, M.D., Kennedy Krieger Institute, 707 N. Broadway, 500i, Baltimore, MD 21205, Fatemi@kennedykrieger.org, Phone: 443 923 2750; Fax: 443 923 2775.

Conflicts of Interest: None

effects on oligodendroglia even months after the initial insult. Despite limited GRP-survival, behavioral and neuropathological outcomes were improved after GRP-transplantation. Our results suggest that exogenous GRPs improve myelination through trophic effects in addition to differentiation into mature oligodendrocytes.

Keywords

Cell Therapy; Cerebral Palsy; Ischemia; Myelination

INTRODUCTION

Approximately two percent of all children born in the United States between 2001–2010 were born very preterm (www.marchofdimes/peristats), and 5–20% of these infants develop spastic cerebral palsy(Hamrick et al. 2004; Marret et al. 2013). An additional 25–50% experience attention deficit disorder, learning disabilities, or visual cortical impairments(Litt et al. 2005), and they have a higher incidence of psychiatric morbidities(Johnson 2007). Neonatal white matter injury (NWMI) is the predominant cause of brain injury in this population(Volpe 2009; Volpe et al. 2011). The period of highest risk for NWMI is between approximately 23 and 32 weeks post-conception age(Volpe 2009). Epidemiological and pathological studies suggest a strong role of perinatal inflammation and perfusion deficits in NWMI(Leviton et al. 2010; O'Shea et al. 2009), and it is postulated that these stressors along with developmentally dependent cell-specific vulnerability of oligodendroglia result in NWMI. In the early stages of injury, NWMI can be distinguished pathologically by the presence of numerous active microglia within the periventricular white matter(Volpe 2003) along with a 50%-90% depletion of oligodendrocyte progenitor cells (OPC) and immature oligodendrocytes(Back et al. 2001; Back et al. 2007). These cells represent the predominant oligodendroglial developmental stage during the peak period of NWMI(Back et al. 2007). There is also evidence that surviving immature oligodendroglia undergo a maturational arrest in NWMI lesions(Billiards et al. 2008; Buser et al. 2012; Fancy et al. 2014). At later stages, NWMI lesions show astrogliosis and extensive myelin pallor along with axonal spheroids(Folkerth 2005). In comparison to these human studies, we have previously shown that CD1 mice with neonatal unilateral carotid artery ligation at P5 show increased apoptosis of oligondedrocyte progenitor cells (OPC) during the acute stages after injury leading to an acute transient drop in OPC counts (Fatemi et al. 2011). While OPC counts recovered after 48 hours, we had shown that OPCs in injured mice expressed a more immature morphology suggesting arrested differentiation (Falahati et al. 2013), and animals with this form of injury exhibited myelin pallor during adulthood (Fatemi et al. 2011).

As of today, the only intervention known to reduce the incidence of cerebral palsy in the preterm population is the use of Magnesium Sulfate given to pregnant mothers with anticipated preterm labor(Cahill et al. 2010). The lack of any disease modifying intervention in patients with NWMI underscores the need for novel therapeutic strategies.

Human glial restricted precursor cells (GRPs) can be derived from fetal brain and spinal tissue (Campanelli et al. 2008; Dietrich et al. 2002; Phillips et al. 2012; Rao and Mayer-Proschel 1997). Several centers and companies have established manufacturing protocols for

these cells and transplantation of these cells is currently being debated as a therapeutic strategy in a number of neurologic diseases, including spinal cord injury, multiple sclerosis, transverse myelitis, leukodystrophies, amyotrophic lateral sclerosis, and cerebral palsy(Goldman et al. 2006). Preclinical studies have been conducted in several white matter disease and other CNS disease models and while several studies have shown a beneficial effect in some of these models(Kim et al. 2012b; Lepore et al. 2011; Maragakis et al. 2005; Walczak et al. 2011), the mechanisms of action of these cells remain somewhat elusive. The objective of this study was to determine the survival, migration and differentiation capacity of GRPs as well as the efficacy of GRP transplantation for improving neurobehavioral and neuropathological outcomes in a previously published mouse model of NWMI(Fatemi et al. 2011).

MATERIALS AND METHODS

Animals

This study was approved by the Johns Hopkins Animal Care and Use Committee (protocol no. MO09M422). Newborn litters of CD-1 mice were purchased from Charles River Laboratories (Wilmington, MA, USA) for induction of white matter injury. The day of birth was defined as P1. For GRP derivation, a colony of C57BL/6-Tg(UBC-GFP)30Scha/J mice (Jackson Laboratories, Bar Harbor, Maine) was established. These mice express enhanced Green Fluorescent Protein (eGFP) under the direction of the human ubiqutin C promoter in all tissues.

GRP Derivation

Timed pregnant eGFP-transgenic mice were euthanized at E13.5 and cells were derived from embryonic spinal cord and grown in a defined ‘GRP’ medium as previously published(Phillips et al. 2012). Briefly, it contains DMEM/F12 1:1 (Invitrogen), B27(50X; Invitrogen), N2 (100X; Invitrogen), Bovine Serum Albumin (BSA; 0.5%), FGF-2 (10–20 ng/ml; Invitrogen) and heparin (1μg/ml;Sigma). Further selection was performed by immunopanning with an A2B5 antibody (Millipore) as previously published(Phillips et al. 2012). For the transplantation procedure, cells were suspended in normal saline and kept on ice for a maximum period of 3 hours prior to transplantation.

Carotid Artery Ligation

On P5, CD-1 pups were placed in an incubator at 35°C for 15 to 30 minutes and were then anesthetized with isoflurane (4% induction 1% to 1.2% maintenance), and the right common carotid artery was ligated (right hemisphere referred to as ipsilateral, left hemisphere as contralateral). Pups recovered at 36°C for 30 to 60 minutes and were returned to the dam. Rectal temperatures were 36°C±0.5°C before surgery and 34.5°C±1°C postoperatively; surgery time was standardized to 12 to 15 minutes. We have shown previously that standardizing the surgery time with this procedure in the CD-1 strain at P5 results in selective white matter injury.(Fatemi et al. 2011)

GRP Transplantation

On P22, animals were anesthetized again with isoflurane (2 min induction at 4% then 1.5% for maintenance) and placed in a stereotaxic device. Hair on scalp was gently shortened using dissection scissors, a small incision was made to the scalp and a 5 microliter Hamilton syringe with 31 gauge needle was inserted through the skull at 1 mm lateral, 3.3 mm anterior to lambda with a depth of 1.2 mm. 100,000 cells were injected in a volume of 1 microliter over the course of 2 minutes. The needle was then left in place for 4 minutes and then slowly removed over 4 minutes. The total duration of each surgery was between 25–30 minutes.

Neurobehavioral Testing

The behavioral protocols used are standard protocols used at the Johns Hopkins animal behavioral core, we focused our behavioral testing on the following protocols in which we had previously found significant abnormalities in our NWMI mouse model (Breu et al. under review): Novelty-induced activity in open field was measured using two identical activity chambers with infrared beams (San Diego Instruments Inc., San Diego, CA, USA). In 6 consecutive sessions of 5 minutes each, horizontal and vertical activities, stereotypic activities, as well as the time spent in the center or the periphery of the chamber were automatically monitored. Startle reactivity and plasticity to acoustic stimuli were measured in two identical startle chambers (San Diego Instruments Inc., San Diego, CA, USA). To avoid locomotion artifacts, each mouse was restrained in a Plexiglas cylinder (5cm in diameter) that was placed on an accelerometer. A loudspeaker mounted 24cm above the cylinder produced the broadband background noise and acoustic stimuli. The SR-LAB software and interface system controlled start, stop, and quality of acoustic stimuli and recorded movement responses from the accelerometer. The maximum readings within 100-ms after stimulus onset were registered to represent startle amplitudes. Sound levels were measured inside the startle chambers using a digital sound level meter (Realistic, Tandy, Fort Worth, TX, USA). Both accelerometer and sound level meter of each startle chamber were calibrated regularly. After a 5-min acclimatization period to a 70-dB background noise (continuous throughout the session), the presentation of stimuli started with 10 40-ms 120-dB white noise impulses at a 20-s inter-stimulus interval (habituation session). The habituation session was followed by a 5-min resting time without any stimulus. Next, the pre-pulse inhibition (PPI) session started in which the animals were exposed to the following trials: pulse-alone trial (a 120-dB, 100-ms, broadband burst); no-stimulus trial; and five pre-pulse– pulse combinations (pre-pulse–pulse trials) consisting of a 20-ms broadband pre-pulse burst followed by a 120-dB pulse 80 ms later. The amplitudes utilized as pre-pulses were 74, 77, 82, 87, and 91 dB. In each session, mice were exposed to six sets of trials in pseudorandom order. The calculation of differences between pulse-alone trial and pre-pulse trials produced the PPI measures for each animal. The habituation amplitudes and percentage of PPI for each animal were used as the dependent variables in statistical analysis.

Histology

Mice were anesthetized and perfused with phosphate-buffered saline (PBS) and then with 4% paraformaldehyde in phosphate buffer. Brains were post-fixed in PFA for 24 h,

cryoprotected in sucrose and sectioned at 40 μm. Sections were mounted onto 10 slides in a 1 in 10 series, with each slide having sections with 400μm displacement. Sections and images were identified using a standardized numbering system, so that antigen expression in near-adjacent sections of the same animal stained with different antibodies could be correlated. Slides were incubated in blocking solution, followed by primary antibody incubation at 4°C overnight: anti-Platelet Derived Growth Factor Receptor Alpha (PDGFR-a) antibody (BD Pharmingen, San Jose, CA, rat, 1:250), anti-CC1 antibody (Calbiochem, San Diego, CA, mouse, 1:1000) for detection of oligodendrocytes, anti-glial fibrillary acidic protein (GFAP) antibody (Dako, Carpinteria, CA, rabbit, 1:2500) for detection of astrocytes, anti-Ki67 (Abcam, Cambridge, UK, rabbit, 1:500) for visualization of proliferation, anti-myelin basic protein (MBP) antibody (Millipore, mouse, 1:2500) for myelin staining, anti-SMI-32 antibody (Covance, mouse, 1:5000) for detection of non-phsophorylated neurofilament, characteristic of abnormal axons. Fluorescent secondary antibodies labeled with Cy5 (emission spectrum does not overlap with that of GFP) were used to detect co-staining with GFP, and all sections were counterstained with Hoechst 33342. The fluorescence signal strength of GFP was tested by staining slides with an anti-GFP antibody (Life Technologies, rabbit, 1:200) in 5 cell-transplanted animals, and it was determined that endogenous GFP signal was detectable in all anti-GFP stained cells (data not shown). For slides stained for brightfield measurements, biotinylated secondary antibodies were used and the antigen-antibody complex was visualized using an ABC ELITE kit (Vector Labs).

GRP cell survival, migration pattern, and differentiation analysis—Fluorescence images were acquired using the Zeiss Axio Imager M5 microscope with ApoTome functionality using structured illumination to optimize resolution. Using this technique the total exposure of the specimen is slightly greater because the grid projection is typically not completely opaque. However, the resolution is comparable to that achieved by either confocal or deconvolution techniques. To reduce bias due to bleaching of the fluorescent antibody, all images used for analysis were acquired the first time the slides were illuminated under the microscope. Mosaic settings, Z-stack settings, and anatomical regions were defined and set in the microscope software prior to acquisition to reduce illumination time and thereby bleaching, using the robotic microscope controls. Fluorescent channels switched automatically and were acquired sequentially for each field of view, in the same order for each sample. Regions to be acquired were selected based on Hoechst 33342 nuclear staining. All images and channels were post-processed in the Zeiss Axiovision software following standardized protocols for optimal quantification. For estimation of transplanted cell survival, the section showing the injection track was identified, and all GFP + cells of that section and the adjacent anterior and posterior sections were manually counted in three layer z-stack images by two individuals in a blinded fashion. Inter-rater reliability between these individuals was 99.5%. Migration patterns were defined as ‘injection track only’, ‘medial or lateral migration’, and ‘migration to contralateral hemisphere’ and noted for each cell-transplanted animal. For quantification of differentiation capacity of GRPs into oligodendrocytes and astrocytes, mosaic images were taken under a 40x objective of anti-CC1 or anti-GFAP-stained sections, counterstained with Hoechst 33342, that were adjacent to those used for GFP+ cell counts. Within the corpus callosum, GFP+CC1+Hoechst+ and GFP+GFAP+Hoechst+ cells were manually counted,

and the proportion of GFP+ cells that were also CC1+ was determined within outlined areas. There were too few GFP+GFAP+ cells (only 0–2 cells seen on each section) to determine a ratio.

MBP and SMI-32 densitometry and CC1 cell counts—For quantification of MBP and SMI32 immunostaining, semiquantitative densitometry was performed using MCID Core (InterFocus Imaging, Ltd. Cambridge, UK) after calibration with optical density standards, as we have previously reported(Fatemi et al. 2011). Subdivisions of the corpus callosum (right, right periventricular, medial, left, and left periventricular) were manually delineated in three sections, at the level of the anterior commissure, anterior hippocampus, and posterior corpus callosum, as well the left and right fimbriae and the left and right internal capsules (Figure 2). Average density values for each of these areas were calculated in each animal and used for further statistical comparisons. For quantification of mature oligodendrocytes, images were taken under a 40X objective on CC1-stained sections in the same regions. Images were stitched together using the mosaic module of the Zeiss AxioVision software (Zeiss Microimaging, LLC, Thornwood, NY), and threshold-based automated cell counting was performed in MCID, as previously reported.

Statistical analysis

Data is expressed as the mean ± standard error for each group of mice. Unpaired two-tailed t-tests were performed to look for significant differences in cell counts between cell transplanted NWMI and controls mice. ANOVAs were performed to determine effects of treatment on each outcome variable (cell counts, density values, behavioral values) at each time point. Power analysis, using an alpha of 0.05, showed the sample size to be sufficient to achieve a power of >0.8 for all group comparisons. When main effects were significant ($p<0.05$), Tukey's multiple comparison tests were performed to evaluate differences between individual treatment groups, while for the open field testing variables and PPI analysis, the Holm-Sidak method of pairwise multiple comparisons was performed. For all figures $*p < 0.05$, $**p < 0.01$ and $***p < 0.001$. Graphs were plotted and statistics assessed using the program GraphPad Prism 5.0 (GraphPad Software) and IBM SPSS 22.

RESULTS

Post-operative Survival

A total of 88 animals underwent carotid artery ligation with a 95.5% survival rate. Four animals were excluded due to the complete necrosis of the ipsilateral cerebral hemisphere observed after tissue extraction. In a first set of experiments, 29 ligated animals and 34 control animals received cell injections and 14 ligated and 11 controls received saline injection on P22 and post-mortem immunofluorescence and IHC were performed at either P50 (4 weeks post-transplantation) or P78 (eight weeks post transplantation). In a second set of experiments, 6 ligated animals received cell injections, and 6 ligated and 8 naïve controls received saline injections at P22; these mice underwent behavioral testing on P64-P78 (6–8 weeks post-transplantation) and were then euthanized.

Purity of GRPs

The immunopanning procedure for selection of GFP+ GRPs, resulted in 95% (range 92–97%) yield of A2B5 positive cells in the three different batches of cells used for the transplantation experiments (see Figure 1). On average 39% (+/− SD 4.3) of these cells also expressed Nestin. A subset of cells were maintained in culture for a week after immunopanning and became nearly all PDGFR-a positive, indicating differentiation into oligodendrocyte progenitors.

GRP Cell Survival and Migration Patterns in NWMI and in Controls

At four weeks, transplanted GFP+ cells were detected in 13 (86.7%) NWMI mice, and in 16 (88.9%) controls. At eight weeks, transplanted cells were detected only in six (42.9%) of NWMI, while compared to 4 weeks, a comparable number of control animals (13 animals; 81.3%) still showed surviving cells (see Table 1). Figure 3 illustrates the different patterns of cell migration seen in cell-transplanted animals.

Interestingly, at 4 weeks migrating cells were found in the contralateral hemisphere in both NWMI mice and controls. However, the pattern of cell migration at 8 weeks was very different in control and NWMI mice. As shown in table 1, cells migrated to the contralateral side in six (37.5%) control animals at 8 weeks, but no cells were detected in the contralateral hemisphere in any of the NWMI mice.

Overall counts of transplanted GFP+ cell were comparable between NWMI and unligated controls at 4 weeks post-transplantation (Figure 4C). In contrast, the overall number of GFP + cells at 8 weeks was approximately four-fold greater in the control group than in NWMI mice (Figure 4F), which may contribute to the observed difference in migration. In order to confirm that the assessment of cell death was accurate, we stained cell transplanted brain sections which did not show any visible eGFP expression with an anti-eGFP antibody and no staining was seen.

In order to assess proliferation of transplanted cells, we conducted co-staining with Ki67. We did not find any single GFP+ cell that co-stained with Ki67 in both NWMI and controls at 4 and 8 weeks post-transplantation. Ki67 staining was clearly observed in stem cell niches (subventricular and subgranular zones).

Differentiation Capacity of Transplanted Cells

At 8 weeks post-transplantation, 40.6% (SD 33.2%) of the GFP+ cells co-stained with CC1 in NWMI mice, suggesting differentiation into oligodendrocytic phenotype (Figure 5). Furthermore, the percent of GFP+ cells expressing this differentiation marker was comparable in control and NWMI animals (Figure 5E). On the other hand, there was almost no co-staining of GFP+ cells with GFAP, suggesting that these cells rarely differentiate into astrocytes (Figure 5F). As anticipated, a large fraction of the transplanted cells were still expressing PDGFR-a, a marker for OPCs. We observed a trend towards higher fraction of GFP+ cells at OPC stage in NWMI mice (mean 75.1%, SD 21.1) compared to unligated controls (mean 60%, SD 9.1), however it did not gain significance, $t(13)=1.630$, $p = 0.13$. A qualitative assessment of stained sections suggests, that in areas closer to injection tract

(Figure 6A), the fraction of GFP+ cells that were at OPC stage was higher compared to other areas (Figure 6B) which is in line with the finding that transplanted cells migrate less in NWMI mice.

Effect of GRP Transplantation on Neuropathologial Outcome in NWMI

To evaluate axonal pathology and myelination, SMI32 and MBP hemispheric densitometry were performed 4 weeks and 8 weeks after transplantation. At 4 weeks, NWMI mice that received saline injections showed significantly higher SMI32 in both the ipsilateral and contralateral internal capsule compared to controls, while cell-treated NWMI mice showed significantly less SMI32 staining than saline-injected NWMI mice (Figure 7). Furthermore, we stratified the GRP treated NWMI mice based on survival of transplanted cells (NWMI/GRP+: animals that showed GFP positive cells; NWMI/GRP-: animals without any GFP positive cells). Interestingly, cell survival status did not have any effect on the degree of axonal SMI32 staining. At 8 weeks post-transplantation no significant differences were seen in hemispheric SMI32 staining between the three experimental groups. This is consistent with our previous work, where a transient axonopathy was seen following neonatal ischemia.

MBP densitometry 4 weeks post-transplantation showed significant reduced MBP in saline treated NWMI mice compared to controls on the ligated hemisphere, $t(14) = 2.25$, $p < 0.05$, while GRP transplanted NWMI animals were comparable to unligated controls and showed significantly higher MBP expression on the ligated side compared to saline treated NWMI mice, $t(14) = 7.5$, $p < 0.001$. At 8 weeks post-transplantation, densitometry revealed a significant reduction in MBP in both hemispheres in saline-treated NWMI mice, but GRP-treated NWMI mice were comparable to healthy controls (Figure 8). Again, this improvement in myelination at 8 weeks was seen in both NWMI/GRP+ and NWMI/GRP- mice.

Effect of GRP Transplantation on Behavioral Outcomes

NWMI mice displayed a highly abnormal startle response. When administered a 120-dB pulse, NWMI mice exhibited a significantly lower startle amplitude, suggesting a sensorimotor deficit. However, transplantation of GRPs successfully ameliorated this abnormality (Figure 9A). NWMI mice also behaved abnormally in PPI testing. In control mice, startle amplitude decreased as expected with increasing pre-pulse intensity. However, NWMI mice responded similarly in each trial, regardless of pre-pulse intensity, indicative of a neurological abnormality. NWMI mice treated with GRPs responded in a similar fashion to the controls, with startle amplitude decreasing as pre-pulse intensity increases (Figure 9B). There was a significant difference between the three animal groups (repeated measure ANOVA $F(2, 55) = 5.133$, $p < 0.05$) while there was not a statistically significant interaction between each different group and pre-pulse intensity ($p = 0.247$). Tukey's multiple comparison analysis, showed significant differences between control and saline-treated NWMI mice ($p < 0.05$), and between GRP- and saline-treated NWMI mice ($p < 0.01$), while no significant differences were seen between control and GRP-treated NWMI mice. There was no correlation between behavioral outcomes and cell survival or migration

pattern. No significant differences were seen among the three groups in any of the open field testing variables.

DISCUSSION

NWMI is a major medical, social, and economic burden, and while no curative treatment currently exists, cell-based therapy is widely discussed as a treatment option(Phillips et al. 2013). This study is the first to determine the effect of glial restricted precursor cell transplantation in a model of NWMI. In an initial set of experiments, we found that GRP cell survival is diminished in animals with neonatal ischemia compared to controls, even though the intracerebral cell injection was not performed until weeks after the initial ischemic insult. However, despite reduced cell survival in NWMI animals, our results show that the differentiation capacity of transplanted GRP cells into mature oligodendrocytes is comparable between healthy and NWMI mice. Furthermore, we found that GRP transplantation after NWMI can induce dramatic recovery in myelination and reduced axonal injury that is irrespective of long-term GRP cell survival. Finally, in a separate set of animals we demonstrated that GRP transplantation after NWMI prevents the behavioral deficits observed in untreated NWMI mice. We conclude that GRP cell transplantation results in amelioration of NWMI by mechanisms not directly related to long-term survival of the transplanted cells.

The NWMI model used here does not have any evidence of motor deficits. However, the diminished startle amplitude and abnormal pre-pulse inhibition seen in this model, improved significantly with GRP transplantation. This is of great clinical relevance since neurosensory deficits are common and debilitating problems in preterm infants. A study comparing the visual cortex responses in preterm infants with white matter injury found decrease in motion-specific suggesting delayed maturation of cortical motion processing(Birtles et al. 2007). Others have shown, that younger, smaller, preterm infants with a complicated perinatal course are at higher risk for auditory problems and is assumed to be caused by injury in primary auditory pathways or processing(Pettigrew et al. 1988). Another study, involving children born preterm, revealed auditory attention processing deficits suggesting impairment of complex auditory reaction circuits (Dupin et al. 2000).

Since the discovery of GRPs by Rao and Mayer-Proeschl in 1997(Rao and Mayer-Proschel 1997), several studies have examined the effect of transplanting these cells in various CNS disease models(Kim et al. 2012b; Lepore et al. 2011; Maragakis et al. 2005; Noble et al. 2011b; Walczak et al. 2011). GRPs generate both oligodendrocytes and astrocytes following transplantation into brain or spinal cord and do not generate neurons, even when they migrate into such neurogenic zones as the rostral migratory stream and olfactory bulb(Herrera et al. 2001). It has been shown that these cells can differentiate into different types of astrocytes in-vitro(Noble et al. 2011a); GRP cells exposed to bFGF and CNTF differentiated almost entirely into A2B5+ process-bearing astrocytes, and those cells exposed to bone morphogenetic protein-4 (BMP-4) differentiate almost entirely into A2B5- astrocytes with a fibroblast-like morphology(Davies et al. 2008). Interestingly, transplantation of BMP-4-induced astrocytes in a rat model of spinal cord injury led to significant motor recovery, while transplantation of CNTF-induced astrocytes led to

allodynia and no motor recovery (Davies et al. 2008). The same group has also shown that human-derived GRPs (hGRPs) did not result in apparent motor-recovery after spinal cord injury (Davies et al. 2011). Another study using human-derived GRPs treated with the same medium we used in this study showed that transplantation of these cells into rats the immune-deficient shiverer mouse led to extensive remyelination of the CNS (Walczak et al. 2011). In contrast, hGRPs transplanted into focally demyelinated rat spinal cord differentiated mainly into GFAP-positive astrocytes(Walczak et al. 2011); interestingly, despite the lack of remyelination in these rats, the hGRP treated group had improved electrophysiological function. Based on these reports, we anticipated that a large fraction of our transplanted GRPs would become astrocytes in the NWMI group. In contrast, while the cell survival was lower in these animals compared to control, almost no exogenous cells acquired GFAP positivity. A large percentage of the transplanted cells were still expressing the PDGFR-a receptor, which is a marker for oligodenrocyte progenitors, and a substantial fraction of surviving GRPs had differentiated into oligodendrocytes, as illustrated by CC1 co-staining, in both healthy controls and NWMI mice. We did not find any significant differences in terms of differentiation capacity between NWMI mice and controls. A limitation of this study is our inability to determine what percent of the myelin repair observed is due to myelin expression of the transplanted cells as opposed to endogenous cells. Despite an attempt using confocal microscopy of Fluoromyelin™ stained sections, it was impossible to determine whether there was true co-localization of GFP and FluoroMyelin™ in the transplated cells or whether the myelin was being expressed by the processes of adjacent endogenous oligodendrocytes (data not shown). Future studies using a second reporter gene under MBP-promotor in the transplanted cells would allow such determination. While this is clearly a limitation of this study, CC1 is considered to be a mature oligodendrocyte marker, and the fact that the many of the transplanted cells showed extensive long parallel processes that appear to be wrapping axons (as seen in Figures 4, 5 and 6), we suspect that the exogenous cells partially contribute to remyelination by direct differentiation.

The local tissue environment may impact the differentiation potential of transplanted cells. As an example, inflammation caused by the inclusion of a MOG/cytokine component in a rat focal demyelination model may influence the ability of the cells to myelinate(Walczak et al. 2011); yet other studies have shown that inflammation has a pro-myelinating effect in retinal transplants of oligodendrocyte precursors(Setzu et al. 2006). In our study, the fact that GRP survival was significantly higher in control animals suggests that neonatal white matter injury generates a toxic environment that leads to death of transplanted cells; this insult generates a persistent inflammatory response(Falahati et al. 2013) that may contribute to transplanted cell death.

Several studies have shown that while transplanted stem cells or precursor cells may not survive long-term in the host, they exert a beneficial effect in the injury(Kim et al. 2012a; Kim et al. 2012b; Titomanlio et al. 2011). In a study by Titomanlio et al, neurosphere-derived precursors implanted into ibotenate-injured brains of neonatal pups migrated to the lesion site and differentiated into oligodendrocytes and neurons, but ultimately died a few weeks later(Titomanlio et al. 2011). However, despite the limited survival, a reduction in lesion size and an improvement in memory performance were seen in transplanted animals

compared with untreated animals. Another study by Kim H et al showed that human embryonic stem cell-derived oligodendrocyte precursors, transplanted in the ventricles of EAE mice, remained within the cerebroventricular system and did not survive for more than 10 days(Kim et al. 2012a). However, EAE mice that received these cells showed a significant improvement in neurological disability scores compared to that of controls. Our results in NWMI mice are consistent with these other reports that despite limited long-term survival, GRPs are able to exert a beneficial effect. It is quite interesting that this effect was seen even in animals that had no evidence of surviving GRPs at 2 months post-transplant. It is yet to be determined how long the transplanted cells are able to survive and when remyelination is initiated in our model. A potential methodological pitfall in our transplanted cell survival assessment could be the fact that some cells may completely downregulate their eGFP expression, and it is possible that there are more transplanted cells that we are unable to detect. However, given that the cell survival was much higher in control group that was survived for the same duration as the injured mice, it is hard to justify why eGFP expression would only be downregulated in cells transplanted into NWMI mice. Utilization of in vivo bioluminescence studies combined with in vivo MRI cell-tracking studies would allow studying the spatiotemporal relationship between exogenous cell death and remyelination.

Notably, transplanted hESC-derived oligodendrocyte progenitor cells have been shown to restrict infiltrating inflammatory cells within the subarachnoid space(Kim et al. 2012a). The migration of inflammatory cells into the white matter during MS and EAE can be modulated by the microenvironment, including chemokines and adhesion molecules from resident cells and inflammatory cells, and by penetration conditions in the blood-brain barrier and the blood-CSF barrier of the choroid plexus(Chabas et al. 2001; Ransohoff et al. 2003). It has also been shown that transplanted OPCs increase CCL2, CXCL9, CXCL10, sICAM-1, and TIMP-1 in the brain and spinal cord, possibly affecting the migration of inflammatory cells(Kim et al. 2012a). Our previous studies were able to detect microglial activation in some regions of the brain during chronic stages of NWMI(Falahati et al. 2013). So it is possible that the transplanted GRPs improve outcome by modulating the post-ischemic immune response in our NWMI model. Future studies need to determine whether GRPs transplantation modulates a neuroinflammatory response in NWMI mice.

In terms of clinical translation, it is important to note that cell-based therapies are already ongoing in children with a variety of neurologic conditions. Bone marrow and cord blood derived hematopoietic stem cell transplantation is currently standard of care in a number of childhood white matter diseases, such as adrenoleukodystrophy and Krabbe Disease(Prasad and Kurtzberg 2010). Furthermore, two current trials of autologous cord blood cell transplantation are currently underway in patients with cerebral palsy in the U.S. (listing on clinicaltrials.gov: NCT01072370, NCT01147653). Most notably, a recent safety study of intracerebral stem cell transplantation of neural stem cells in boys with the hypomyelinating leukodystrophy, Pelizaeus-Merzbacher disease, was conducted(Gupta et al. 2012).

It is important to note that the prediction of neurologic disability remains a major challenge during the acute phase of perinatal brain injury in prematurely born infants, and the diagnosis of cerebral palsy (CP) is usually not made until 2–3 years of life. Furthermore, many children with CP will significantly improve during the preschool years (Myers and

Ment 2009). Ethical and safety issue are another major concern when it comes to clinical trials in neonates and infants. Therefore, we chose a time point for our cell transplantation experiments, which represents the developmental stage of an older child in whom the diagnosis of cerebral palsy is usually confirmed at a chronic disease stage. It is well known that many stem cells have the potential for tumorigenesis. For this reason, limited survival of donor cells with long-term neurological recovery, as seen in this current study, is highly desirable in terms of overall safety.

Future studies need to identify the bioactive molecules that are released by transplanted GRPs, which could serve as novel therapeutic modalities. It is also important that the behavioral improvements following GRP transplantation, as observed in this study, are reproduced in other animal models of NWMI and by other laboratories, before proceeding with the path towards clinical trials using GRPs in neonatal white matter injury.

Acknowledgment

This project was funded by the National Institute of Health K08-NS063956 (AF), R01- NS33958 (J.D.R.), 5P30HD024061-25 (M.V.J., A.W.P.), and the Child Neurology Foundation.

ABBREVIATIONS

bFGF	basal Fibroblast Growth Factor
CNTF	Ciliary Neurotrophic Factor
EAE	Experimental Allergic Encephalitis
eGFP	enhanced Green Fluorescence Protein
GFAP	Glial Fibrillary Acidic Protein
GRP	Glial Restricted Precursor
MBP	Myelin Basic Protein
NWMI	Neonatal White Matter Injury
OPC	Oligodendrocyte Progenitor Cell
PDGFR-a	Platelet Derived Growth Factor Receptor - Alpha
PPI	Pre-Pulse Inhibition

REFERENCES

Back SA, Luo NL, Borenstein NS, Levine JM, Volpe JJ, Kinney HC. Late oligodendrocyte progenitors coincide with the developmental window of vulnerability for human perinatal white matter injury. J Neurosci. 2001; 21:1302–1312. [PubMed: 11160401]

Back SA, Riddle A, McClure MM. Maturation-dependent vulnerability of perinatal white matter in premature birth. Stroke. 2007; 38:724–730. [PubMed: 17261726]

Billiards SS, Haynes RL, Folkerth RD, Borenstein NS, Trachtenberg FL, Rowitch DH, Ligon KL, Volpe JJ, Kinney HC. Myelin abnormalities without oligodendrocyte loss in periventricular leukomalacia. Brain Pathol. 2008; 18:153–163. [PubMed: 18177464]

Birtles DB, Braddick OJ, Wattam-Bell J, Wilkinson AR, Atkinson J. Orientation and motion-specific visual cortex responses in infants born preterm. Neuroreport. 2007; 18:1975–1979. [PubMed: 18007197]

Buser JR, Maire J, Riddle A, Gong X, Nguyen T, Nelson K, Luo NL, Ren J, Struve J, Sherman LS. Arrested preoligodendrocyte maturation contributes to myelination failure in premature infants. Ann Neurol. 2012; 71:93–109. and others. [PubMed: 22275256]

Cahill AG, Stout MJ, Caughey AB. Intrapartum magnesium for prevention of cerebral palsy: continuing controversy? Curr Opin Obstet Gynecol. 2010; 22:122–127. [PubMed: 20179596]

Campanelli JT, Sandrock RW, Wheatley W, Xue H, Zheng J, Liang F, Chesnut JD, Zhan M, Rao MS, Liu Y. Expression profiling of human glial precursors. BMC Dev Biol. 2008; 8:102. [PubMed: 18947415]

Chabas D, Baranzini SE, Mitchell D, Bernard CC, Rittling SR, Denhardt DT, Sobel RA, Lock C, Karpuj M, Pedotti R. The influence of the proinflammatory cytokine, osteopontin, on autoimmune demyelinating disease. Science. 2001; 294:1731–1735. and others. [PubMed: 11721059]

Davies JE, Proschel C, Zhang N, Noble M, Mayer-Proschel M, Davies SJ. Transplanted astrocytes derived from BMP- or CNTF-treated glial-restricted precursors have opposite effects on recovery and allodynia after spinal cord injury. J Biol. 2008; 7:24. [PubMed: 18803859]

Davies SJ, Shih CH, Noble M, Mayer-Proschel M, Davies JE, Proschel C. Transplantation of specific human astrocytes promotes functional recovery after spinal cord injury. PLoS One. 2011; 6:e17328. [PubMed: 21407803]

Dietrich J, Noble M, Mayer-Proschel M. Characterization of A2B5+ glial precursor cells from cryopreserved human fetal brain progenitor cells. Glia. 2002; 40:65–77. [PubMed: 12237844]

Dupin R, Laurent JP, Stauder JE, Saliba E. Auditory attention processing in 5-year-old children born preterm: evidence from event-related potentials. Dev Med Child Neurol. 2000; 42:476–480. [PubMed: 10972420]

Falahati S, Breu M, Waickman AT, Phillips AW, Arauz EJ, Snyder S, Porambo M, Goeral K, Comi AM, Wilson MA. Ischemia-induced neuroinflammation is associated with disrupted development of oligodendrocyte progenitors in a model of periventricular leukomalacia. Dev Neurosci. 2013; 35:182–196. and others. [PubMed: 23445614]

Fancy SP, Harrington EP, Baranzini SE, Silbereis JC, Shiow LR, Yuen TJ, Huang EJ, Lomvardas S, Rowitch DH. Parallel states of pathological Wnt signaling in neonatal brain injury and colon cancer. Nat Neurosci. 2014; 17:506–512. [PubMed: 24609463]

Fatemi A, Wilson MA, Phillips AW, McMahon MT, Zhang J, Smith SA, Arauz EJ, Falahati S, Gummadavelli A, Bodagala H. In vivo magnetization transfer MRI shows dysmyelination in an ischemic mouse model of periventricular leukomalacia. J Cereb Blood Flow Metab. 2011; 31:2009–2018. and others. [PubMed: 21540870]

Folkerth RD. Neuropathologic substrate of cerebral palsy. J Child Neurol. 2005; 20:940–949. [PubMed: 16417840]

Goldman SA, Lang J, Roy N, Schanz SJ, Sim FS, Wang S, Washco V, Windrem MS. Progenitor cell-based myelination as a model for cell-based therapy of the central nervous system. Ernst Schering Res Found Workshop. 2006:195–213. [PubMed: 16903424]

Gupta N, Henry RG, Strober J, Kang SM, Lim DA, Bucci M, Caverzasi E, Gaetano L, Mandelli ML, Ryan T. Neural stem cell engraftment and myelination in the human brain. Sci Transl Med. 2012; 4 155ra137 and others.

Hamrick SE, Miller SP, Leonard C, Glidden DV, Goldstein R, Ramaswamy V, Piecuch R, Ferriero DM. Trends in severe brain injury and neurodevelopmental outcome in premature newborn infants: the role of cystic periventricular leukomalacia. J Pediatr. 2004; 145:593–959. [PubMed: 15520756]

Herrera J, Yang H, Zhang SC, Proschel C, Tresco P, Duncan ID, Luskin M, Mayer-Proschel M. Embryonic-derived glial-restricted precursor cells (GRP cells) can differentiate into astrocytes and oligodendrocytes in vivo. Exp Neurol. 2001; 171:11–21. [PubMed: 11520117]

Johnson S. Cognitive and behavioural outcomes following very preterm birth. Semin Fetal Neonatal Med. 2007; 12:363–373. [PubMed: 17625996]

Kim H, Walczak P, Kerr C, Galpoththawela C, Gilad AA, Muja N, Bulte JW. Immunomodulation by transplanted human embryonic stem cell-derived oligodendroglial progenitors in experimental autoimmune encephalomyelitis. Stem Cells. 2012a; 30:2820–2829. [PubMed: 22949039]

Kim H, Walczak P, Muja N, Campanelli JT, Bulte JW. ICV-transplanted human glial precursor cells are short-lived yet exert immunomodulatory effects in mice with EAE. Glia. 2012b; 60:1117–1129. [PubMed: 22499166]

Lepore AC, O'Donnell J, Kim AS, Williams T, Tuteja A, Rao MS, Kelley LL, Campanelli JT, Maragakis NJ. Human glial-restricted progenitor transplantation into cervical spinal cord of the SOD1 mouse model of ALS. PLoS One. 2011; 6:e25968. [PubMed: 21998733]

Leviton A, Allred EN, Kuban KC, Hecht JL, Onderdonk AB, O'Shea TM, Paneth N. Microbiologic and histologic characteristics of the extremely preterm infant's placenta predict white matter damage and later cerebral palsy. the ELGAN study. Pediatr Res. 2010; 67:95–101. [PubMed: 19745780]

Litt J, Taylor HG, Klein N, Hack M. Learning disabilities in children with very low birthweight: prevalence, neuropsychological correlates, and educational interventions. J Learn Disabil. 2005; 38:130–141. [PubMed: 15813595]

Maragakis NJ, Rao MS, Llado J, Wong V, Xue H, Pardo A, Herring J, Kerr D, Coccia C, Rothstein JD. Glial restricted precursors protect against chronic glutamate neurotoxicity of motor neurons in vitro. Glia. 2005; 50:145–159. [PubMed: 15657939]

Marret S, Marchand-Martin L, Picaud JC, Hascoet JM, Arnaud C, Roze JC, Truffert P, Larroque B, Kaminski M, Ancel PY. Brain injury in very preterm children and neurosensory and cognitive disabilities during childhood: the EPIPAGE cohort study. PLoS One. 2013; 8:e62683. and others. [PubMed: 23658763]

Myers E, Ment LR. Long-term outcome of preterm infants and the role of neuroimaging. Clin Perinatol. 2009; 36:773–789. vi. [PubMed: 19944835]

Noble M, Davies JE, Mayer-Proschel M, Proschel C, Davies SJ. Precursor cell biology and the development of astrocyte transplantation therapies: lessons from spinal cord injury. Neurotherapeutics. 2011a; 8:677–693. [PubMed: 21918888]

Noble M, Mayer-Proschel M, Davies JE, Davies SJ, Proschel C. Cell therapies for the central nervous system: how do we identify the best candidates? Curr Opin Neurol. 2011b; 24:570–576. [PubMed: 22027545]

O'Shea TM, Allred EN, Dammann O, Hirtz D, Kuban KC, Paneth N, Leviton A, Investigators Es. The ELGAN study of the brain and related disorders in extremely low gestational age newborns. Early Hum Dev. 2009; 85:719–725. [PubMed: 19765918]

Pettigrew AG, Edwards DA, Henderson-Smart DJ. Perinatal risk factors in preterm infants with moderate-to-profound hearing deficits. Med J Aust. 1988; 148:174–177. [PubMed: 3277017]

Phillips AW, Falahati S, DeSilva R, Shats I, Marx J, Arauz E, Kerr DA, Rothstein JD, Johnston MV, Fatemi A. Derivation of glial restricted precursors from E13 mice. J Vis Exp. 2012

Phillips AW, Johnston MV, Fatemi A. The potential for cell-based therapy in perinatal brain injuries. Transl Stroke Res. 2013; 4:137–148. [PubMed: 23814628]

Prasad VK, Kurtzberg J. Cord blood and bone marrow transplantation in inherited metabolic diseases: scientific basis, current status and future directions. Br J Haematol. 2010; 148:356–372. [PubMed: 19919654]

Ransohoff RM, Kivisakk P, Kidd G. Three or more routes for leukocyte migration into the central nervous system. Nat Rev Immunol. 2003; 3:569–581. [PubMed: 12876559]

Rao MS, Mayer-Proschel M. Glial-restricted precursors are derived from multipotent neuroepithelial stem cells. Dev Biol. 1997; 188:48–63. [PubMed: 9245511]

Setzu A, Lathia JD, Zhao C, Wells K, Rao MS, Ffrench-Constant C, Franklin RJ. Inflammation stimulates myelination by transplanted oligodendrocyte precursor cells. Glia. 2006; 54:297–303. [PubMed: 16856149]

Titomanlio L, Bouslama M, Le Verche V, Dalous J, Kaindl AM, Tsenkina Y, Lacaud A, Peineau S, El Ghouzzi V, Lelievre V. Implanted neurosphere-derived precursors promote recovery after neonatal excitotoxic brain injury. Stem Cells Dev. 2011; 20:865–879. and others. [PubMed: 20964621]

Volpe JJ. Cerebral white matter injury of the premature infant-more common than you think. Pediatrics. 2003; 112:176–180. [PubMed: 12837883]

Volpe JJ. The encephalopathy of prematurity--brain injury and impaired brain development inextricably intertwined. Semin Pediatr Neurol. 2009; 16:167–178. [PubMed: 19945651]

Volpe JJ, Kinney HC, Jensen FE, Rosenberg PA. The developing oligodendrocyte: key cellular target in brain injury in the premature infant. Int J Dev Neurosci. 2011; 29:423–440. [PubMed: 21382469]

Walczak P, All AH, Rumpal N, Gorelik M, Kim H, Maybhate A, Agrawal G, Campanelli JT, Gilad AA, Kerr DA. Human glial-restricted progenitors survive, proliferate, and preserve electrophysiological function in rats with focal inflammatory spinal cord demyelination. Glia. 2011; 59:499–510. and others. [PubMed: 21264955]

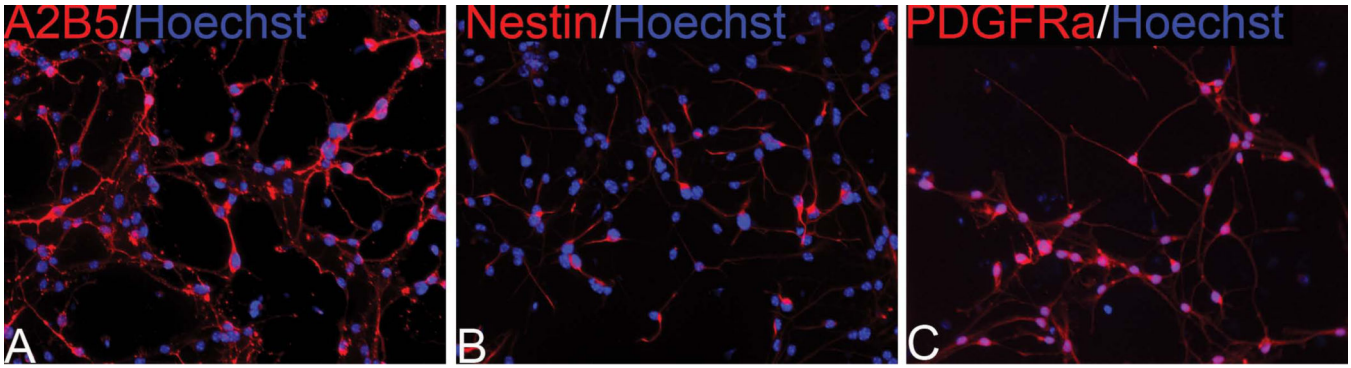

Figure 1.

In vitro assessment of Glial Restricted Precursors (GRPs): Cells were derived at E13.5 and maintained in GRP culture. Cells were confirmed to be GRPs by their expression of A2B5 (A). As previously reported about 40% of the cells expressed Nestin (B). A week after culturing these immunopanned cells, almost all cells were PDGFR-a positive (C).

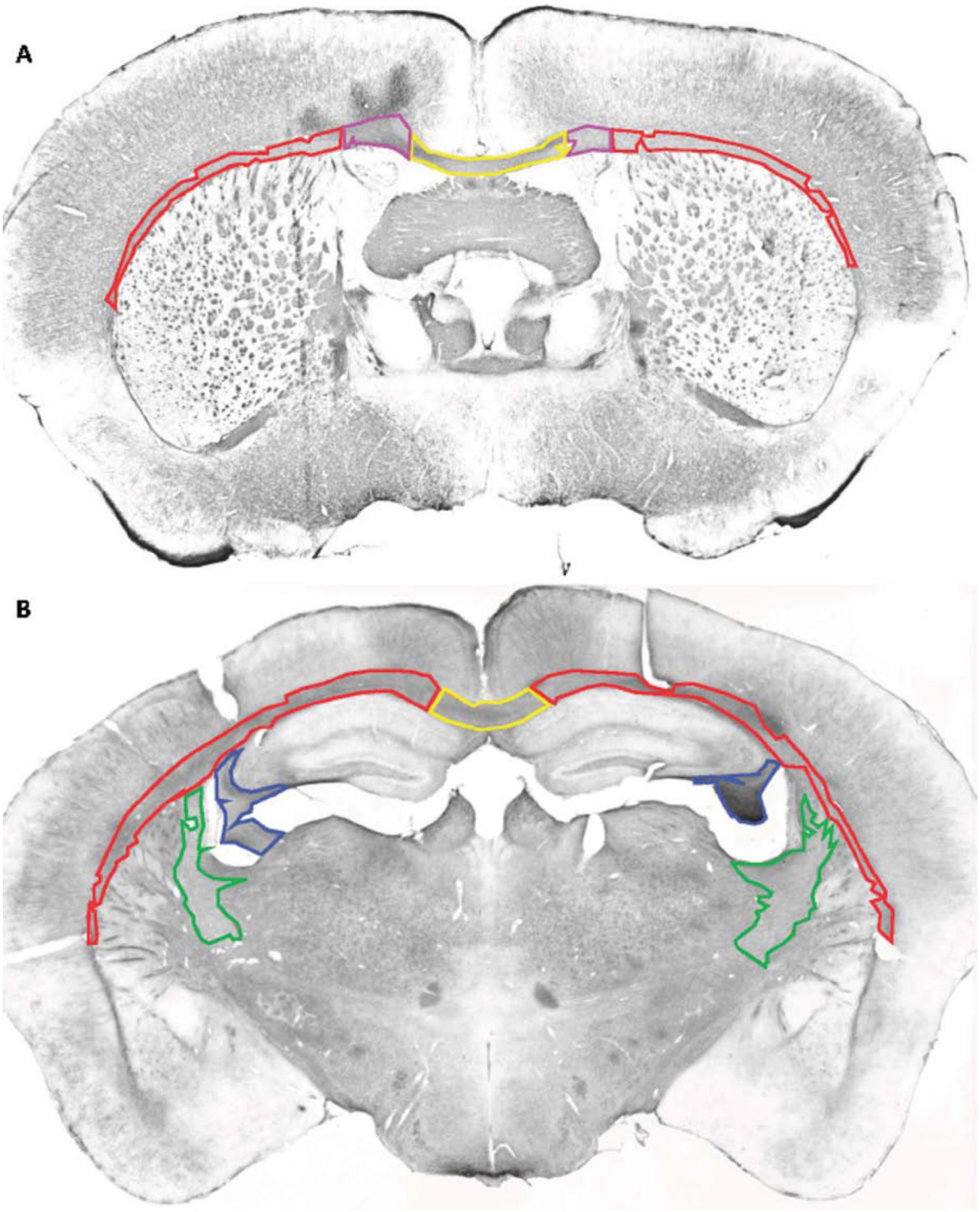

Figure 2. Regions of interest for densitometric analysis

In anterior and medial coronal sections (A), the lateral corpus callosum (red), the periventricular corpus callosum (purple), and the mid corpus callosum (yellow) were assessed. In posterior sections (B), in addition to the lateral (red) and medial (yellow) corpus callosum, the fimbriae of the hippocampus (blue) and the internal capsules (green) were also analyzed. Anterior section was 600 microns anterior to injection site (3.9 mm anterior to lambda), and posterior section is was 400 microns posterior to injection site (2.9 mm anterior to lambda).

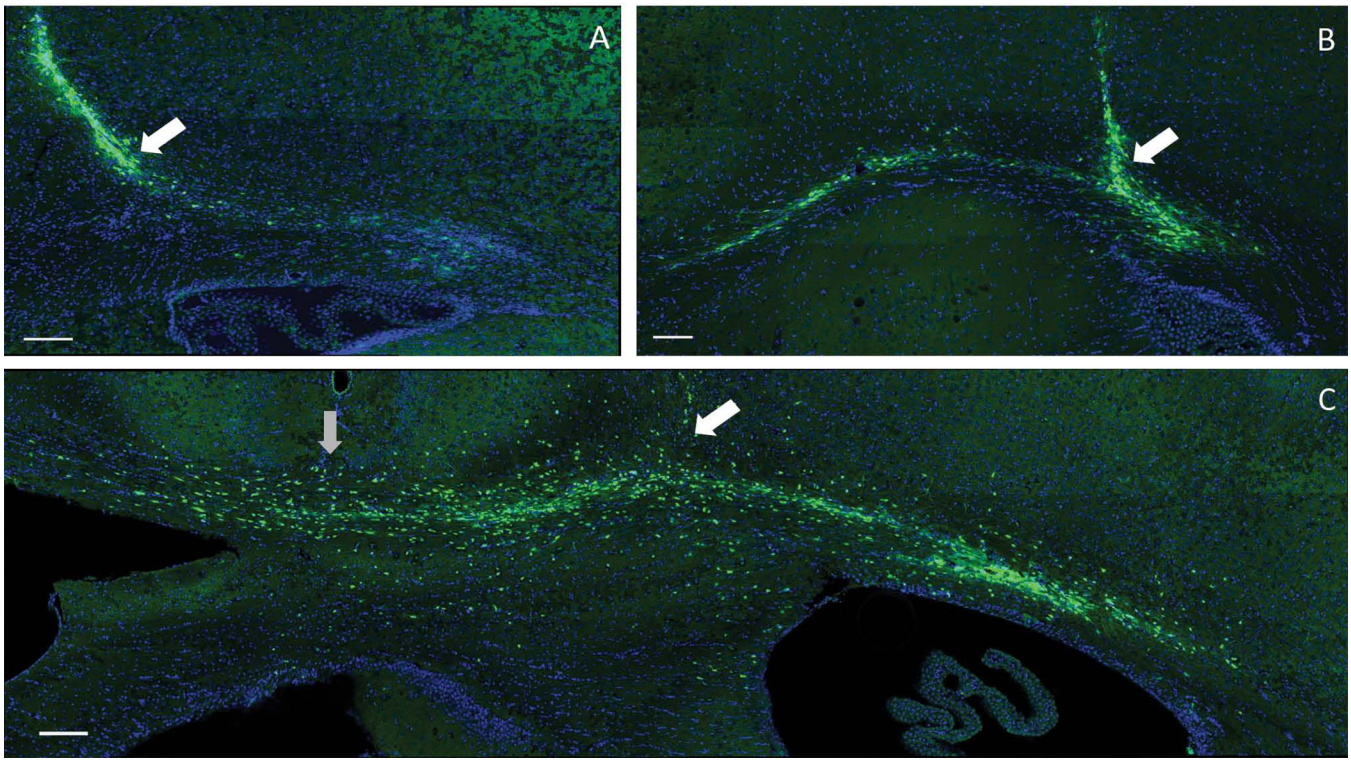

Figure 3. Patterns of Migration of transplanted GRPs

While in some animals transplanted cells remained mostly limited within the injection track (A), robust migration medially and laterally was observed frequently (B, C). Cell Migration to contralateral hemisphere was observed in controls at 2 months but not in NWMI mice. White oblique arrows point to injection site, vertical gray arrow points at the midsagittal line. Scale bar 100 μm.

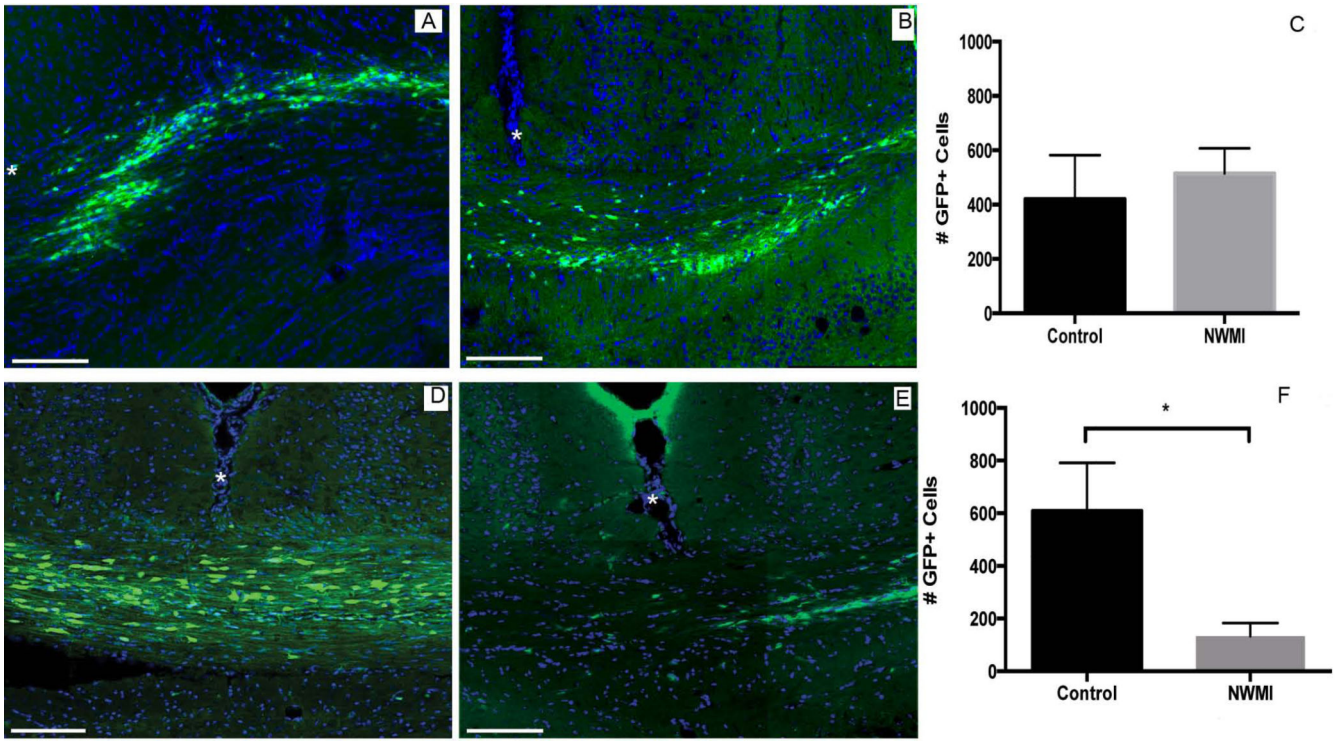

Figure 4. GRP cell survival at 1 month and 2 months post-transplantation

At 1 month, both groups showed comparable number of surviving cells (A, B, C). However, at 2 months post-transplantation control mice (D) had significantly more surviving GFP+ cells when compared to NWMI mice (E, F, $t(28)=2.33$, $p = 0.02$). Plots (C, F) show total number of cells counted in three sections, the one where the injection tract was most prominent, and the immediate anterior and posterior sections. Error Bar indicates 1SE. Scale bar 100 μm.

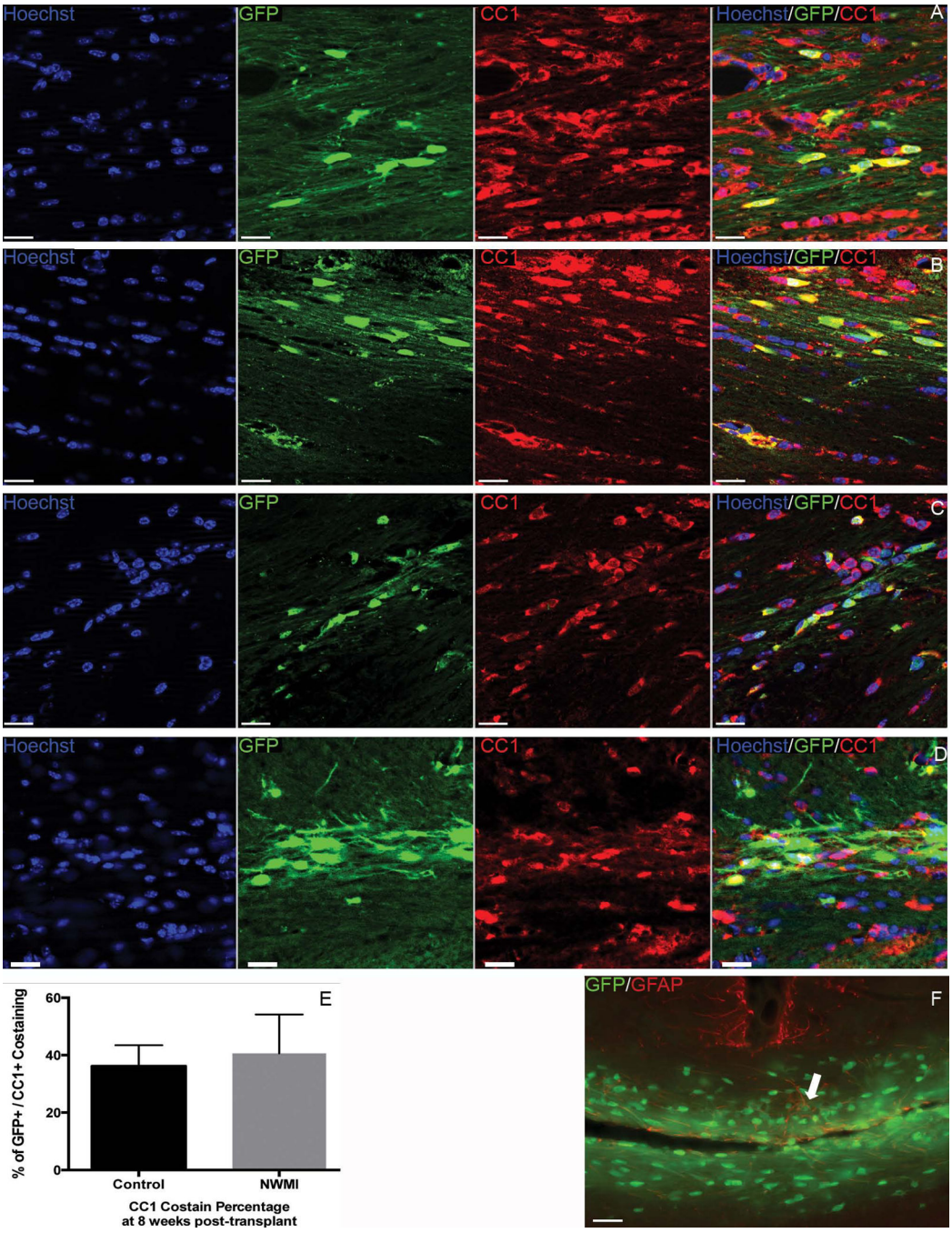

Figure 5. Differentiation capacity of transplanted GRPs

A large fraction of surviving GFP+ cells co-expressed CC1, a marker for mature oligodendrocytes, in two control animals (A, B) as well as in two NWMI (C, D) mice. There was no significant difference in the percentage of CC1+/GFP+ cells between controls and NWMI mice (E), unpaired t-test $t(16) = 0.32$. Little to no GFAP costaining was observed except in a handful cells (arrow, F) suggesting that only a very small fraction of these cells differentiated into astrocytes. Scale bar 20 μm. Error Bar indicates 1SE.

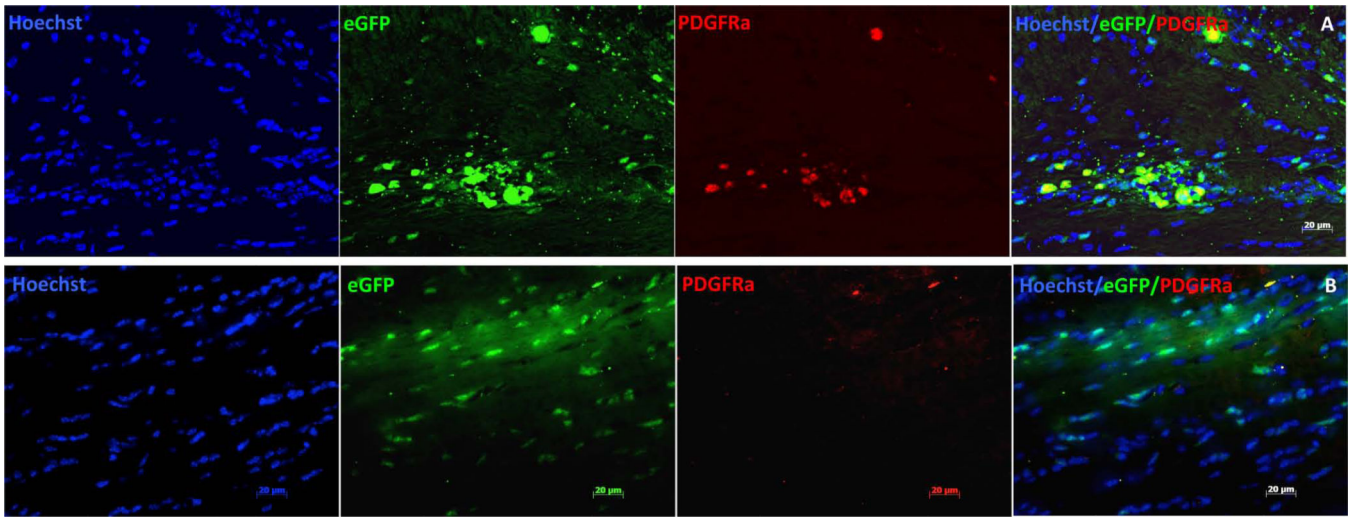

Figure 6. Many transplanted cells Remain as oligodendrocyte progenitor cells (OPCs)

PDGFR-a staining, as an OPC marker, conducted at 2 months post-GRP transplantation showed that a large fraction of transplanted cells remain as progenitor cells. A qualitative assessment of stained sections suggests, that in areas closer to injection tract (A), the fraction of GFP+ cells that were at OPC stage was higher compared to other areas (B).

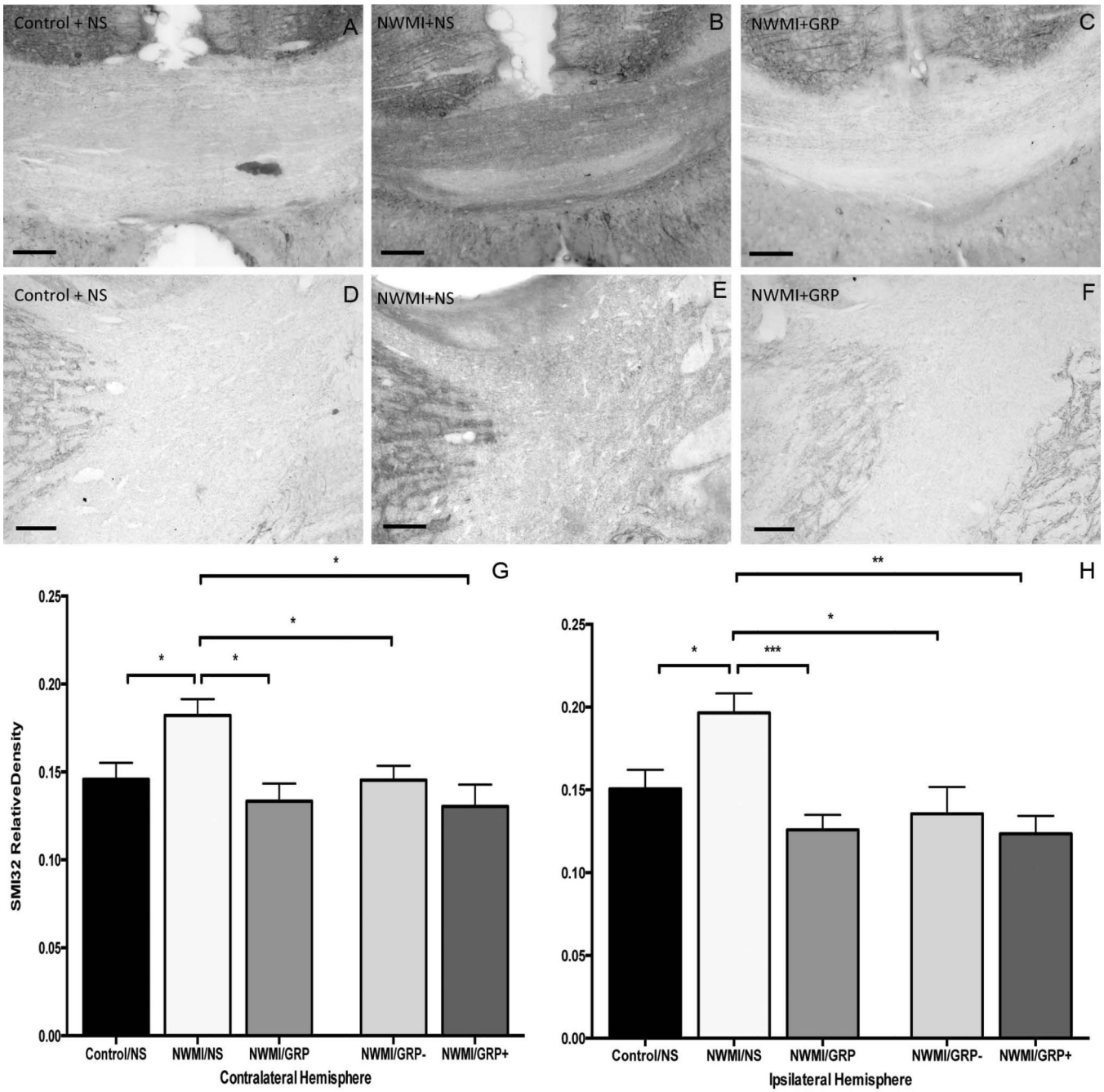

Figure 7. Effect of GRP transplantation on axonal injury

At 4 weeks post-transplantation, there was a significant difference in degree of pathological axonal staining between the different animal groups; ANOVA for ligated hemisphere F (2, 21) = 9.093, $p < 0.01$; for contralateral hemisphere F (2, 21) = 3.939, $p < 0.05$. Saline treated NWMI mice had significantly higher degree of pathological SMI32 staining in both hemispheres as shown in corpus callosum (A–C) and internal capsule (D–F). Treatment with GRPs prevented the increase in SMI32 staining (C,F). Furthermore, we stratified the GRP treated NWMI mice based on survival of transplanted cells (NWMI/GRP+: animals that

showed GFP positive cells; NWMI/GRP-: animals without any GFP positive cells). To our great surprise, cell survival did not correlate with outcome (G–H), and whether transplanted cells had survived (NWMI/GRP+) or died (NWMI/GRP-), a comparable ameliorative effects was observed at 4 weeks in GRP treated animals. Scale bar 50 μm. Tukey's multiple comparison tests p values are shown as * for $p < 0.05$, ** for $p < 0.01$, and *** for $p < 0.001$.

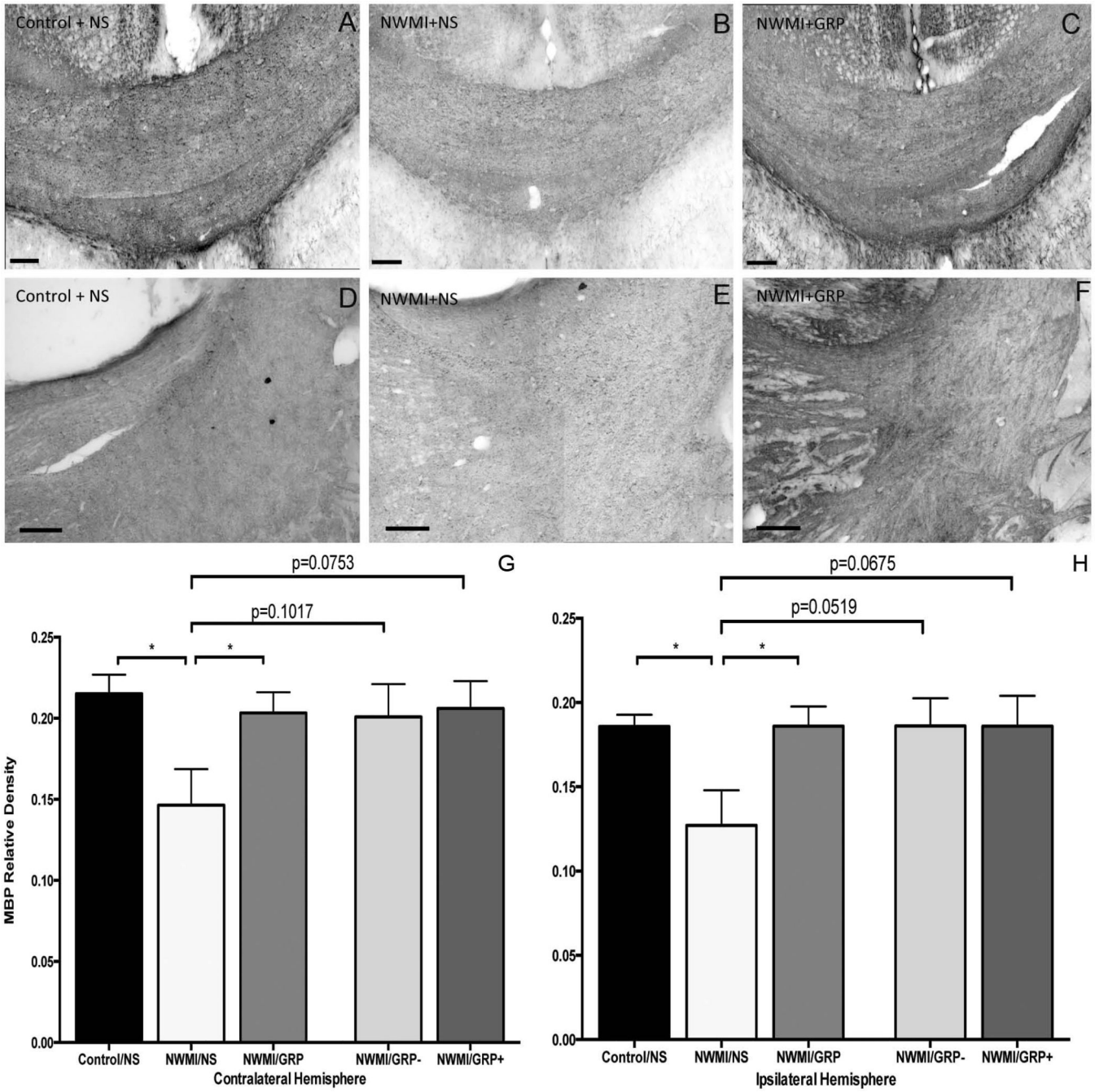

Figure 8. Effect of GRP transplantation on Myelination

At 8 weeks post-transplantation, there were significant differences in hemispheric MBP density values between the different groups; ANOVA for ligated hemisphere F (2, 25) = 4.922, $p < 0.05$; ANOVA for contralateral hemisphere F (2, 25) = 4.356, $p < 0.05$. Saline-treated NWMI mice had significantly lower hemispheric MBP staining as shown in the mid corpus callosum (A–C) and the internal capsule (D–F) when compared to controls, while GRP treated NWMI mice showed comparable MBP densities as in controls (C and F). As seen with SMI32 staining, cell survival did not correlate with outcome (G–H), and whether

transplanted cells survived (NWMI/GRP+) or died (NWMI/GRP-), animals that had no surviving exogenous cells still showed the same amount of recovery as those that did have surviving cells. This recovery showed a trend that did not gain significance when broken down by cell survival status. Scale bar 50 μm. Tukey's multiple comparison tests *p* values are shown as * for $p < 0.05$, ** for $p < 0.01$, and *** for $p < 0.001$.

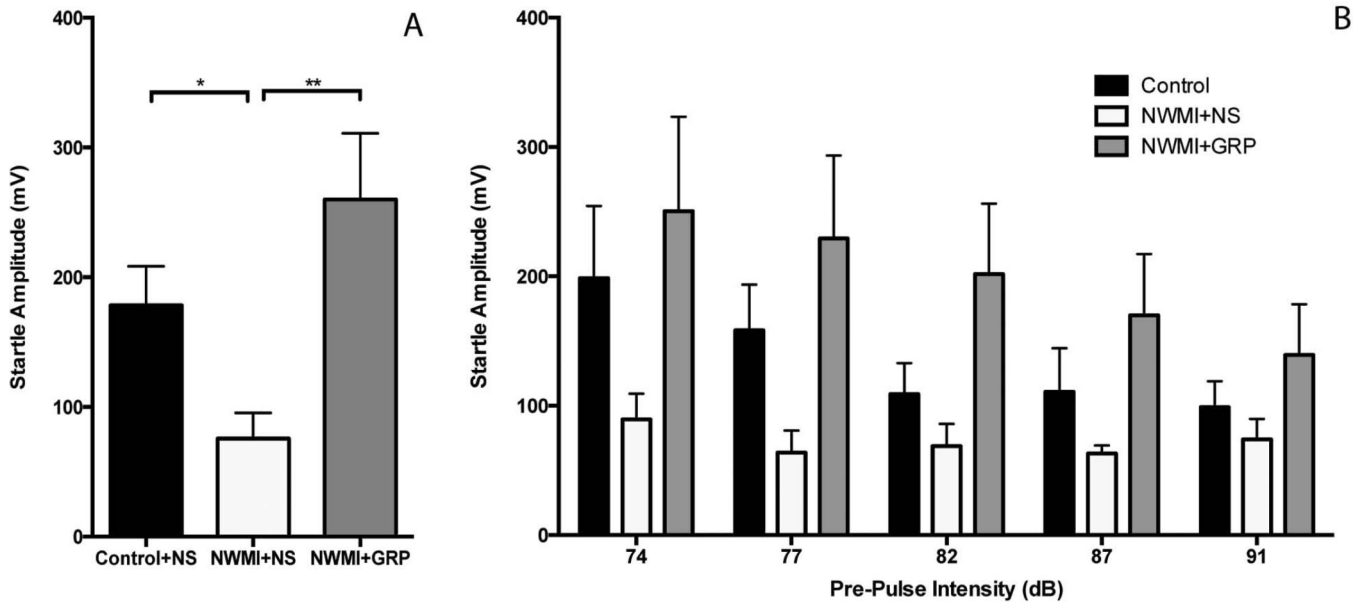

Figure 9. Effect of GRP transplantation on neurobehavioral outcome

There was a significant difference in the startle response between the animal groups, ANOVA $F(2, 87) = 14.057$, $p < 0.001$. The saline treated NWMI group had severely diminished startle response while this deficit was fully reversed by GRP transplantation (A). Prepulse Inhibition (PPI) testing showed again significant difference between the animal group (B); repeated measure ANOVA $F(2, 55) = 5.133$, $p < 0.05$. Again the saline treated NWMI group showed reduced amplitudes and diminished habituation to pre-pulse intensity change, while these deficits were fully reversed in the GRP treated group. Tukey's multiple comparison analysis showed significant differences between control and saline-treated NWMI mice ($p < 0.05$), and between GRP- and saline-treated NWMI mice ($p < 0.01$), while no significant differences were seen between control and GRP-treated NWMI mice. Post-hoc multiple comparison tests p values shown as * for $p < 0.05$, ** for $p < 0.01$, and *** for $p < 0.001$.

Table 1

Patterns of Migration of Transplanted GRPs assessed at 4 and 8 weeks post-transplantation in control and NWMI mice.

Patterns Observed	4 weeks post-GRP transplant		8 weeks post-GRP transplant	
	Control	NWMI	Control	NWMI
Animals with GFP+ GRPs Total	16/18 (88.9%)	13/15 (86.7%)	13/16 (81.3%)	6/14 (42.9%)
Animals with GFP+ GRPs remaining in injection track	5/18 (27.8%)	5/15 (33.3%)	2/16 (12.5%)	2/14 (14.3%)
Average cell count (+/−1SD)	118(+/−48)	154(+/−90)	74 & 83	154 & 172
Animals with GFP+ GRPs migrating along corpus callosum	11/18 (61.1%)	8/15 (53.3%)	11/16 (68.8%)	4/14 (28.6%)
Average cell count (+/−1SD)	320(+/−153)	586(+/−343)	527(+/−278)	255 (+/− 150)
Animals with GFP+ GRPs crossing midline to contralateral hemisphere	3/18 (16.7%)	2/15 (13.3%)	6/16 (37.5%)	0/14 (0%)
Average cell count (+/−1SD)	973(+/−402)	755 & 1077	1245(+/−816)	none